

**PETROGRAPHY AND METALLOGRAPHIC COOLING RATE OF H-CHONDRITE IMPACT MELT BRECCIA LAP 04751.** Elizabeth A. Frank<sup>1</sup>, Axel Wittmann<sup>2</sup>, and David A. Kring<sup>2</sup>, <sup>1</sup>Dept. of Earth & Environmental Sciences, Rensselaer Polytechnic Institute, Troy, NY 12180 (franke2@rpi.edu). <sup>2</sup>Lunar and Planetary Institute, Houston, TX 77058.

**Introduction:** Impact melts resulting from crater-producing impacts on asteroids can be used to understand the collisional evolution of our solar system. Part of that analysis includes an assessment of the cooling rates of the impact melts and/or the locations where the melts are deposited. In this study, we examined LAP 04751 [1], which is an impact melt breccia that came from the H-chondrite parent body.

**Petrography:** Thin section LAP 04751,6 is composed of 54% impact melt (7.3 % in quenched zones around clasts) and 46% surviving clasts. A detailed point count (1742 pts with a spacing of 100  $\mu\text{m}$ ) of the melt indicates the silicate matrix (66.9% of the melt) entrains orbicular metal and sulfide (16.7% of the melt; Fig. 1) and small ( $\leq 310 \mu\text{m}$ ) silicate xenocrysts and xenoliths (12.7% of melt) that also survived the impact. Fractures and holes (3.7%) are randomly distributed through the melt.

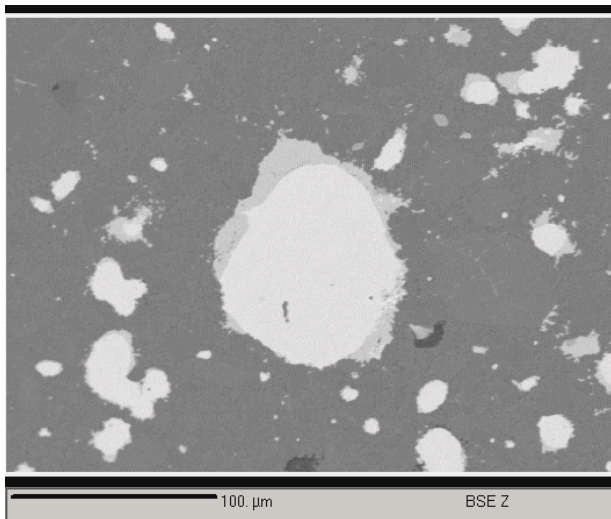


Figure 1: BSE image of metal orb in melt. The dark gray phase is silicate material; intermediate gray indicates sulfide; and light gray metal.

The surviving clasts have Type 4 thermal metamorphic characteristics [2]: (a) some brown glass is preserved in barred olivine chondrules; (b) microcrystalline radial pyroxene chondrule fragments occur with a wide variety of low- to high-Ca pyroxene compositions; (c) feldspar was not found as grains larger than  $\sim 20 \mu\text{m}$ .

The impact melt is very fine-grained ( $< 4 \mu\text{m}$  in average size). Isolated fragments of olivine ( $\text{Fa}_{17-18}$ ) and pyroxene ( $\text{En}_{84-85}\text{Fs}_{14-15}\text{Wo}_{1.1-1.5}$ ) in a remnant feldspathic mesostasis have compositions that match those of H-

chondrites. These small olivine and pyroxene clasts incorporated in the impact melt exhibit a wide range of shock metamorphic features as would be expected in an impact melt breccia. Olivine ubiquitously exhibits planar fractures, undulous extinction, and mosaicism, which suggests shock pressures up to  $\sim 50 \text{ GPa}$  (shock stages S2-S4 after [3]). No high-pressure polymorphs or diaplectic glass were identified, possibly due to elevated post-shock temperatures. Nonetheless, the presence of bulk impact melt suggests shock pressures  $> 80 \text{ GPa}$  and a minimum post-shock temperature increase of  $1500 \text{ }^\circ\text{C}$  [3].

As seen in Figure 2, metal and sulfide particle sizes range from  $\leq 1$  to  $\sim 300 \mu\text{m}$ . The smallest ( $\leq 1 \mu\text{m}$ ) particles are in zones of melt quenched against the clasts. Most of the remaining particles are in the 32 to 59  $\mu\text{m}$  range, which is smaller than that seen in the Orvinio impact melt breccia [4]. The size distribution is not bimodal, like that seen in the Cat Mountain impact melt breccia [5]. These comparisons imply the impact-dispersed metal in LAP 04751 did not have as much time to reconstitute into larger particles and, thus, that the melt initially cooled faster initially than either Orvinio or Cat Mountain.

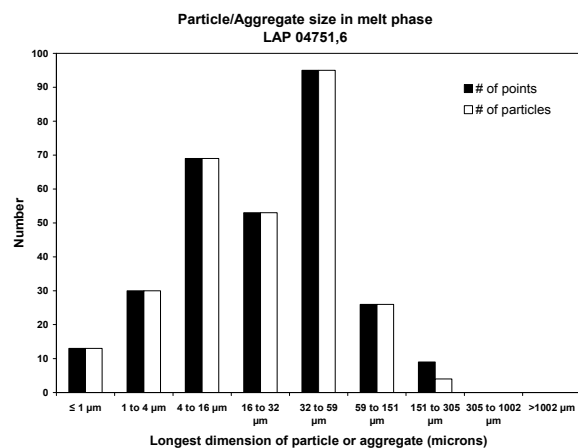


Figure 2: Point count results of metal and sulfide phase distributions.

**Cooling Rates:** LAP 04751 reflects two stages of cooling, which is characteristic of impact melts. During Stage 1, superheated impact melt thermally equilibrates with relatively cool clastic material. During Stage 2 cooling, the subsolidus breccia of melt and clasts cools at a slower rate to the surroundings, which may be the rest of the asteroid and/or space,

depending on whether it is buried or deposited on the planetesimal's surface.

**Stage 1 Fast Cooling:** To determine the initial phase of cooling, we examine the nucleation and growth of metal particles using the method of [6]. The faster the cooling rate, the fewer crystal nuclei form and the greater the distance is between them. As such, the spacings between individual metal particles can be used to determine the Stage 1 cooling rate [6]. Based on 18 spacings that ranged from 22 to 34  $\mu\text{m}$ , the cooling rate was between 19.2 and 67.8  $^{\circ}\text{C}/\text{s}$ , or  $\sim 50$   $^{\circ}\text{C}/\text{s}$ . This range is similar to those of H-type chondrites Dimmit, Pulsora, Tell, Tynes Island, Weston [6], and type-H chondrite impact melt breccia LAP 02240 [7].

**Stage 2 Slow Cooling:** Nickel gradients and subsolidus crystallization in the metal orbs are reflections of the Stage 2 cooling rate of a melt. If samples of melt are buried sufficiently deep and cooled sufficiently slow, secondary kamacite rims around the orbs can crystallize, providing a quantitative means of determining the cooling rate, as seen in the Cat Mountain [5] and Shaw [6] impact melt breccias. In contrast, the orbs in LAP 04751 do not have any secondary kamacite rims, indicating a faster cooling rate (Fig. 3).

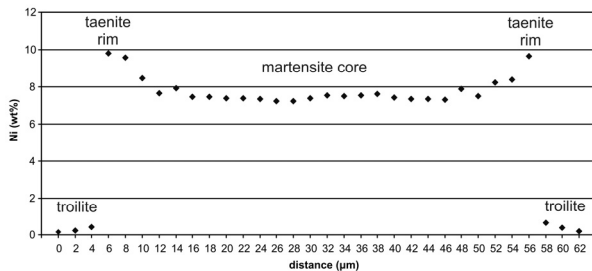


Figure 3: Typical Ni profile across metal-sulfide particle. In this case, the maximum metal core to rim Ni gradient is  $\sim 3$  wt%.

In this case, diffusion gradients between the core and rim of an orb can be used to semi-quantitatively determine the cooling rate. This method has previously been used with Ramsdorf, Orvinio, and LAP 02240 [4, 8, 7]. However, the Ni gradient in LAP 04751, is shallower and of a smaller range than those seen previously. The relative Ni gradients in Ramsdorf vary between from 8 to 20 wt% [4]; those of Orvinio are 1 to 8 wt% [8]; and those of LAP 02240 are 2 to 6 wt% [7], while those of LAP 04751 are from 1 to 4 wt%.

The relative Ni gradient in Ramsdorf was previously compared to experimentally heat-treated samples, from which a cooling rate of  $\sim 10^{-3}$   $^{\circ}\text{C}/\text{s}$  was inferred [8]. A similar comparison of Orvinio's Ni gradients to the those of heat-treated samples implied a slightly slower cooling rate, closer to  $10^{-3}$  to  $10^{-4}$   $^{\circ}\text{C}/\text{s}$  [4]. Likewise, the Ni gradient in LAP 02240 was used to infer a cooling rate of  $10^{-3}$  to  $10^{-4}$   $^{\circ}\text{C}/\text{s}$  [7].

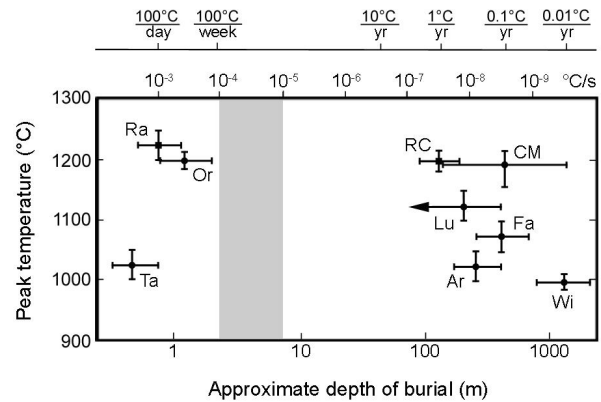


Figure 4: Approximate depth of burial plot. Plotted points: Ramsdorf (Ra), Orvinio (Or), Tadjera (Ta), Rose City (RC), Lubbock, (Lu), Farmington (Fa), Arapahoe (Ar), and Wickenburg (Wi). The estimated cooling rate range for LAP04751 is shaded in gray. Diagram is modified from [5,8].

The range of the relative Ni gradients in LAP 04751 overlaps those of Orvinio and LAP 02240, from which we infer a similar ( $10^{-3}$  to  $10^{-4}$   $^{\circ}\text{C}/\text{s}$ ), if not slightly slower ( $10^{-4}$  to  $10^{-5}$   $^{\circ}\text{C}/\text{s}$ ) cooling rate (Fig. 4). This cooling rate suggests the melt was buried at a depth less than 10 m, likely as ejecta or the uppermost part of a melt breccia lens within a crater.

**References:** [1] Satterwhite C. and Righter K. (2007) *Ant. Met. Newslet.* 30, (1) p. 15. [2] van Schmus W.R. and Wood J.A., (1967) *GCA*, 31, 747-765. [3] Stöffler D. et al. (1991), *GCA* 55, 3845-3867. [4] Taylor, J.G. and Heymann, D. (1971) *JGR*, 76, 1879-1893. [5] Kring D.A. et al. (1996) *JGR.*, 101, 29,353-29,371. [6] Scott E.R.D. (1982) *GCA*, 46, 813-823. [7] Cheek C.C. and Kring D.A. (2008) *LPSC* 39, abstract #1169. [8] Smith B.A. and Goldstein J.I. (1977) *GCA*, 41, 1061-1072.